Probing the Mechanism of Proton Coupled Electron Transfer to Dioxygen: the Oxidative Half-Reaction of Bovine Serum Amine Oxidase†

Qiaojuan Su and Judith P. Klinman*

Department of Chemistry, University of California, Berkeley, California 94720

Received May 12, 1998; Revised Manuscript Received June 23, 1998

ABSTRACT: Bovine serum amine oxidase (BSAO) catalyzes the oxidative deamination of primary amines, concomitant with the reduction of molecular oxygen to hydrogen peroxide via a ping-pong mechanism. A protocol has been developed for an analysis of chemical and kinetic mechanisms in the conversion of dioxygen to hydrogen peroxide. Steady-state kinetics show that two groups need to be deprotonated to facilitate the oxidative half-reaction. The pH dependence of $V_{max}/K_m(O_2)$ reveals pK_a's of 6.2 ± 0.3 and 7.0 ± 0.2, respectively. A pK_a of 7.2 ± 0.1 has been obtained from a titration of anaerobically reduced BSAO using UV−vis spectrophotometry. The near identity of the pK_a obtained from the reduced enzyme titration with the second pK_a from steady-state kinetics suggests that this second pK_a arises from the reduced cofactor. The assignment of pK_a is supported by the observed pH dependence for formation of the cofactor semiquinone signal, detected by EPR spectroscopy under anaerobic conditions. To address the nature of rate-limiting steps in the oxidative half-reaction, the solvent isotope effect, viscosity effect, and O-18 isotope effect on $V_{max}/K_m(O_2)$ have been determined. The solvent isotope effect is indistinguishable from unity, ruling out a proton transfer as a rate-determining step. Use of glucose as a solvent viscosogen shows no viscosity effect, indicating that binding of oxygen is not in the rate-determining step. The O-18 kinetic isotope effect is independent of pH with an average value of $^{18}(V/K) = 1.0097 \pm 0.0010$. This has been compared to calculated equilibrium O-18 isotope effects for various dioxygen intermediate species [Tian and Klinman (1993) *J. Am. Chem. Soc. 115*, 8891], leading to the conclusion that either the first electron transfer to dioxygen or the desorption of product peroxide from a Cu(II)−OOH complex could be the rate-limiting step. The distribution of steady-state enzyme species was, therefore, analyzed through a combination of stopped-flow experiments and analysis of ^{D}V and $^{D}(V/K)$ for benzylamine oxidation. We conclude that the major species accumulating in the steady state are the oxidized cofactor−substrate Schiff base complex and the reduced, aminoquinol form of cofactor. These data rule out a slow release of product hydroperoxide from the aminoquinone form of enzyme, leading to the conclusion that the first electron transfer from substrate-reduced cofactor to dioxygen is the rate-determining step in the oxidative half-reaction. This step is also estimated to be 40% rate-limiting in k_{cat}. An important mechanistic conclusion from this study is that dioxygen binding is a separate step from the rate-limiting electron-transfer step to form superoxide. On the basis of a recently determined X-ray structure for the active form of a yeast amine oxidase from *Hansenula polymorpha* [Li et al. (1998) *Structure 6*, 293], a hydrophobic space has been identified near the O-2 position of reduced cofactor as the putative dioxygen binding site. Movement of superoxide from this site onto the Cu(II) at the active site may occur prior to further electron transfer from cofactor to superoxide.

Bovine serum amine oxidase (BSAO)[1] is a copper-containing enzyme (EC 1.4.3.6) that catalyzes a two-electron oxidative deamination of primary amines concomitant with the two-electron reduction of oxygen to hydrogen peroxide. The reaction has been shown to go through a ping-pong mechanism (*1*), illustrated in eqs 1 and 2:

$$E_{ox} + RCH_2NH_3^+ \rightarrow E_{red}-NH_3^+ + RCHO \quad (1)$$

$$E_{red}-NH_3^+ + O_2 + H_2O \rightarrow E_{ox} + H_2O_2 + NH_4^+ \quad (2)$$

Copper amine oxidases are homodimers containing a topa quinone (TPQ) cofactor (*2*) and a copper ion within each subunit. The crystal structures of amine oxidases from *Escherichia coli* (*3*), pea seedling (*4*), *Arthrobacter globiformis* (*5*), and the yeast *Hansenula polymorpha* (*6*) have been solved. There is considerable structural homology among these amine oxidases: The copper ion is coordinated by three histidine side chains and two water ligands in an approximately square-pyramidal arrangement. The TPQ cofactor is adjacent to the copper site, and is connected to the copper ion through a hydrogen-bonding network involving a number of active-site water molecules (*6*). There is

† This research was supported by grants from the National Institutes of Health, GM 39296 and GM 25765.

* To whom correspondence should be addressed. J.P.K. is also in the Department of Molecular and Cell Biology at the University of California, Berkeley.

[1] Abbreviations: BSAO, bovine serum amine oxidase; TPQ, topa quinone; TPQ_{red}, topa quinone in the reduced form; TPQ_{ox}, topa quinone in the oxidized form; TPQ_{sq}, topa semiquinone; HPAO, *Hansenula polymorpha* amine oxidase.

S0006-2960(98)01103-9 CCC: $15.00
Published on Web 08/18/1998

Scheme 1: Proposed Mechanism for the Reductive Half-Reaction

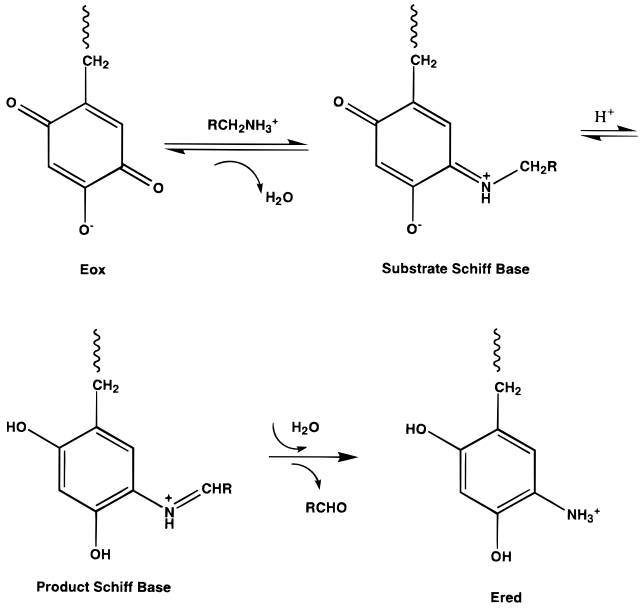

also a conserved aspartate residue, on the opposite side of the TPQ from the copper center, which has been implicated as an obligatory base in substrate oxidation (*3*, *7*). The mechanism of the reductive half-reaction is fairly clear (*8*), as summarized in Scheme 1. Similar to other aminotransferase mechanisms (*9*), a substrate Schiff base complex is generated upon formation of a covalent adduct at the C-5 position of the TPQ cofactor with the amine substrate. This is followed by proton abstraction from the C-1 of substrate by the active-site base, to yield reduced cofactor in a product Schiff base complex. Finally, the product Schiff base is hydrolyzed to release an aldehyde, leaving the reduced TPQ cofactor in its aminoquinol form. Although initial crystal structures did not reveal a pathway for substrate to reach the TPQ from solvent, more recent structures indicate a substrate binding channel quite clearly (*5*, *6*). The degree of rate limitation by the various steps in the reductive half-reaction is dependent on the source of the copper amine oxidase. In the case of BSAO, substrate deuterium isotope effects indicate that proton abstraction is either partially or fully rate-determining.

In contrast to detailed studies of the reductive half-reaction, little has been known about the oxidative half-reaction, eq 2. Inhibition of the amine oxidases by copper chelates with superoxide dismutase activity suggested that superoxide was likely to be an intermediate in dioxygen reduction (*10*). It has been proposed that copper is required for the oxidative half-reaction, on the basis of the inhibition of enzyme activity by copper ligands (*11*) and of the observation that enzyme forms that contain a reduced, quinol form of cofactor but lack a redox active metal fail to undergo reoxidation in air to topa quinone (*12*). The detection of a Cu(I)−semiquinone by EPR after reduction of enzyme with amine substrate under anaerobic conditions has led to the suggestion that Cu(I) plays the key catalytic role in the oxidative half-reaction (*13*). Temperature-jump experiments indicate that formation of the Cu(I)−semiquinone species is sufficiently fast to place this intermediate on the catalytic pathway (*14*).

The oxidative half-reaction of amine oxidases involves a two-proton and two-electron transfer from the reduced enzyme to dioxygen. The TPQ cofactor can be thought of as a "transducer" molecule that stores both protons and electrons obtained from substrate until the aldehyde product dissociates and dioxygen binds. There are fundamental questions that need to be addressed regarding the "linkage" between the reductive and oxidative halves of the reaction. For example, what is the prototropic form of cofactor that initiates its oxidation? Where does the dioxygen interact with the cofactor/copper center and what is the nature of the rate-determining step for conversion of dioxygen to hydrogen peroxide? Finally, what is the exit channel for loss of product peroxide from the enzyme and how does this relate spatially to the substrate binding channel? Answering these questions can provide important insights into the strategies used by enzymes to catalyze a two-electron reduction of dioxygen to hydrogen peroxide. In particular, we would like to understand how these enzymes facilitate the reduction of a thermodynamically potent oxidant that behaves in a kinetically sluggish manner, due to its ground-state triplet spin state.

As described in this study, a series of experimental protocols have been developed that allow detailed characterization of the mechanism of dioxygen reduction. This includes kinetic studies to determine whether catalysis is linked to proton donation or loss, together with investigations of O-18 isotope effects, solvent isotope effects, and viscosity effects to address the nature of rate-limiting steps. Ambiguities that arise among alternate kinetic mechanisms may be resolved by a combination of stopped-flow and steady-state studies to identify species that accumulate during steady-state turnover.

EXPERIMENTAL PROCEDURES

Materials. All materials were obtained commercially and were reagent grade unless otherwise indicated. Bovine serum amine oxidase was purified by a modification of the procedure of Summers et al. (*15*). The protein concentration was determined spectrophotometrically at 280 nm using an $E_{1cm}^{1\%}$ of 20.8 (*16*). To eliminate the effect of small fluctuation of enzyme activity, a standard enzyme assay was carried out together with each set of rate measurements. Standard enzyme assays employed 10 mM benzylamine as substrate in 100 mM potassium phosphate buffer, at pH 7.2, 25 °C, and were monitored by the decrease of oxygen concentration. The ratio of the observed rate to 0.36 units/mg provided a correction factor that was then applied to all measurements within a given set.

Benzylamine was obtained from Aldrich and converted to the hydrochloride salt by bubbling HCl(g) through an ethereal solution followed by recrystallization 2 times from methanol. [1,1-$^2H_2$] benzylamine was synthesized following the procedure described by Bardsley et al. (*17*).

Methods. Steady-State Kinetics. Initial velocity studies for the oxidation of [1,1-$^1H_2$] and [1,1-$^2H_2$] benzylamine were carried out at 25 °C by monitoring oxygen consumption on a Yellow-Springs oxygen monitor. Different oxygen concentrations were achieved by flowing the appropriate O_2/N_2 gas mixture into the space between the assay solution (1 mL) and the oxygen probe for 5−10 min. The initial oxygen

concentration was recorded when equilibrium was reached after the oxygen probe had been placed in the assay solution. Assay solutions below pH 8 contained 100 mM potassium phosphate; those above pH 8 contained 25 mM potassium pyrophosphate. The ionic strength was adjusted to 0.3 M by addition of NaCl. Steady-state parameters were obtained by nonlinear fit of data to the Michaelis−Menten equation using the program KaleidaGraph on a Macintosh computer.

Titration of Reduced Enzyme. A series of 14.8 μM BSAO solutions were prepared by adding 50 μL of 12.6 mg/mL BSAO stock solution to 412.5 μL of buffer (buffer contained 100 mM potassium phosphate, pH below 8, or 25 mM potassium pyrophosphate, pH above 8). Glucose and catalase were added to the solution for a final concentration of 50 mM glucose and 52 units/mL of catalase. Each BSAO solution (485 μL) was purged with argon in a sealed cuvette for 30 min before the injection of a small volume (5 μL) of glucose oxidase stock solution (not subjected to anaerobiosis) to attain a final concentration of 50 units/mL of glucose oxidase. A benzylamine solution was also flushed with argon (for 15 min) prior to injection of 10 μL to yield a final solution volume of 500 μL. The reduced enzyme solution was kept anaerobic under the extra pressure provided by an argon balloon. Spectra were obtained at 25 °C on a Hewlett-Packard 8452A UV−vis photodiode array spectrophotometer. Spectra of the oxidized and reduced enzyme were taken before and after addition of benzylamine, respectively.

pH Dependence of Topa Semiquinone Formation. A concentrated, pH 7.2, BSAO solution (~2 mM) was made from a 17.4 mg/mL stock solution, using a Collodion vacuum concentrator (Schleicher and Schuell). This concentrated BSAO solution was divided into 10 μL aliquots and mixed with equal volumes of 100 mM potassium phosphate buffer at various pH values. The final pH values were determined as 6.59, 6.79, 6.90, 7.00, 7.12, 7.29, 7.43, and 7.59 in a separate set of mixing experiments without enzyme but on a scale suitable for pH measurements using 10 mL of pH 7.2 buffer and 10 mL of various pH buffers. A set of 100 mM benzylamine solutions was prepared in 100 mM potassium phosphate buffers with pH values adjusted to the above listing. Both the BSAO samples and the corresponding benzylamine solutions were purged with argon for 20 min before being placed in an anaerobic glovebox. Benzylamine solutions (10 μL) were then added to the 20 μL BSAO samples. About 5 μL of the resulting, substrate-reduced BAO sample was transferred to an EPR capillary and sealed with wax. The final concentration of BSAO was about 0.65 mM, and the benzylamine concentration was 33.3 mM. Leftover mixtures of BSAO and benzylamine were exposed to air for several hours until the pink color of oxidized BSAO reappeared. These air-oxidized BSAO samples were transferred to separate EPR capillaries, and EPR spectra of both reduced and oxidized BSAO were acquired.

EPR spectra were measured using a Bruker ESP300 EPR spectrometer (Bruker, Germany) equipped with a low-noise microwave amplifier (Mitech) and a loop-gap resonator (Medical Advances). The loop-gap resonator was inserted into a quartz vacuum Dewar, and the temperature was controlled by a Eurotherm B-VT 2000 thermostat to 36.1 ± 0.5 °C. The sweep field was 3124.963−3424.963 G, power 1.01 mW, frequency 9.18 GHz, modulation amplitude 3.32 G, receiver gain 1000. Spectra were the average of 9 scans to obtain a better signal-to-noise ratio.

Solvent Isotope Effect. The enzyme solution was lyophilized and dissolved in D_2O twice to remove H_2O. Substrate solutions contained benzylamine, NaCl, and potassium phosphate buffer. Dry components were dissolved in D_2O, and the pD was adjusted with KOD. This initial solution was then lyophilized and redissolved in D_2O twice. The final pD value was remeasured using a regular pH electrode by adding 0.4 to the meter reading (*18*). The steady-state kinetics were carried out at a range of pD values.

Viscosity Effect. Viscosity studies were performed at pH 6.5, with 18.4 mM benzylamine in 100 mM potassium phosphate buffer, ionic strength 0.3 M. Buffer and substrate solutions were prepared in the presence of glucose as a viscosogen. With glucose concentrations of 0, 8, 14, 22, 26, and 30 wt %, the relative viscosities were 1, 1.25, 1.5, 2, 2.5, and 3, respectively, at 20 °C (*19*). Steady-state measurements were carried out at 25 °C as described under steady-state kinetics.

O-18 Isotope Effects. O-18 kinetic isotope effects were measured at 20 °C, pH 6.0, 7.2, and 8.5, buffered by 100 mM potassium phosphate or 25 mM potassium pyrophosphate, with 1 mM O_2 and saturating benzylamine at each pH. The reaction was coupled with horseradish peroxidase using guaiacol as substrate in order to convert H_2O_2 to H_2O; this step was necessary to prevent any nonenzymatic disproportionation of H_2O_2 to O_2 and H_2O. O-18 effects were measured by a competitive method using natural abundance O-18. The experimental apparatus was described previously (*20*). The remaining O_2 in the reaction mixture was isolated from the solution and converted to CO_2. The pressure of CO_2 was measured and compared to the CO_2 pressure from the blank to determine the extent of reaction f. The CO_2 was trapped and sealed in a glass tube, which was then sent to Krueger Enterprises in Cambridge, MA, for analysis of the isotope ratio ($R = {}^{18}O/{}^{16}O$) by mass ratio spectrometry. The O-18 isotope effect was calculated according to

$$^{18}(V/K) = 1/(1 + \ln(R/R_0)/\ln(1 - f)) \qquad (3)$$

where R_0 is the isotope ratio of the blank.

Stopped-Flow Kinetics. Stopped-flow experiments were carried out at 25 °C in 100 mM potassium phosphate buffer, pH 6.5, on an Applied Photophysics Limited Model SF.17MV stopped-flow spectrophotometer interfaced with an Acorn Archimedes 420/1 computer. The stopped-flow apparatus was prepared for anaerobiosis using the following procedure: a closed thermostat fluid circuit was set up and connected to a water pump to allow circulation; and helium was bubbled through the water bath thermostat to minimize oxygen concentration in the thermostat fluid and to avoid oxygen diffusion into the sample flow line. Oxygen was removed from BSAO sample by purging with helium for 20 min. Potassium phosphate buffer, benzylamine solution, and 5 mM sodium dithionite solution were made anaerobic by bubbling helium through each solution. The sample flow line was flushed several times with deoxygenated 5 mM sodium dithionite solution, pH 8, and allowed to stand with this sodium dithionite solution for 3 h. Deoxygenated potassium phosphate buffer was then used to wash out the

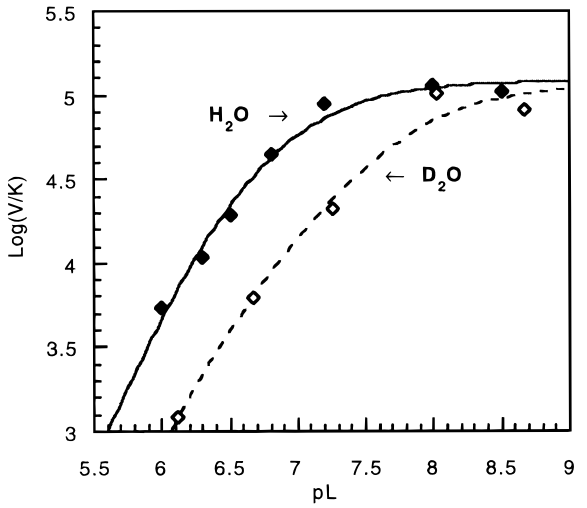

FIGURE 1: pH/pD dependence of $V_{max}/K_m(O_2)$. $V_{max}/K_m(O_2)$ measured in D_2O (open diamonds) is compared to that in H_2O (closed diamonds). Lines are fit to the following equation: $\log(V/K) = \max - \log(1 + 10^{pK_a(2) - pL} + 10^{pK_a(1) + pK_a(2) - 2pL})$. pL represents pH (in H_2O) or pD (in D_2O). The maximum $V_{max}/K_m(O_2)$ is 1.21 $\times$ 10^5 M^{-1} s^{-1} (0.0852 μmol/min·mg·μM) in H_2O and 1.15 $\times$ 10^5 M^{-1} s^{-1} (0.0810 μmol/min·mg·μM) in D_2O.

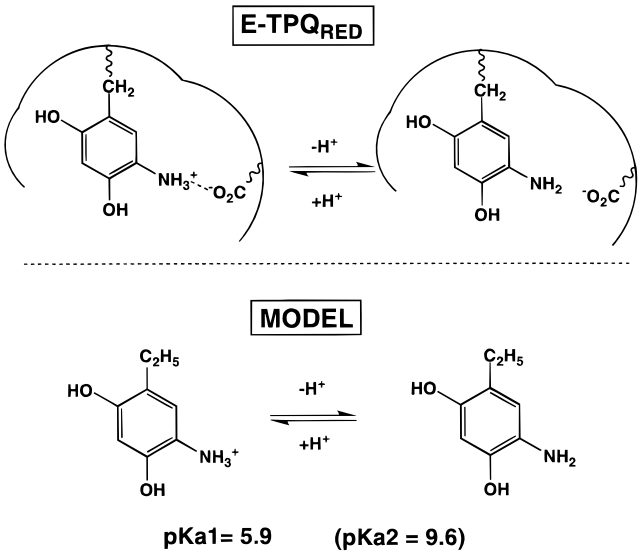

FIGURE 2: Comparison of proton dissociation for the reduced TPQ cofactor in the enzyme and for the model compound. Only the first deprotonation is shown in each case, ascribed to the ionization of the protonated amine, on the basis of the similarity of the reduced cofactor to aniline (*21*). The second pK_a of the model compound is listed from ref *21*.

sodium dithionite solution three times to remove any trace dithionite. Deoxygenated BSAO sample was mixed with deoxygenated benzylamine solution before being transferred to the stopped-flow syringe; a second syringe was filled with air-saturated potassium phosphate buffer. The benzylamine reduced BSAO and oxygenated buffer were rapidly mixed in the stopped-flow apparatus, and the oxidized topa quinone (TPQ_{ox}) absorbance was followed as an increase at 480 nm with time. The final concentrations were the following: BSAO 21.15 μM, benzylamine 10 mM, and oxygen 129 μM. For the aerobic process, the resting enzyme was mixed with benzylamine (both in potassium phosphate buffer), and the decrease in TPQ_{ox} absorbance was followed at 480 nm as a function of time. The traces from both processes could be fit to single-exponential equations.

RESULTS

pH Dependence of $V_{max}/K_m(O_2)$. For a ping-pong mechanism, V_{max}/K_m of the second substrate is independent of parameters in the first half-reaction. Given the ping-pong behavior of BSAO, we have been able to examine steps that involve the binding of O_2 up to the first irreversible step in its conversion to H_2O_2 by measuring $V_{max}/K_m(O_2)$. As shown in Figure 1, $V_{max}/K_m(O_2)$ increases over 1 order of magnitude from pH 6.0 to 8.5. Fitting the data in Figure 1 to an equation with one pK_a is not satisfactory since the observed $V_{max}/K_m(O_2)$ increases faster than that predicted by a single pK_a (result not shown). A two pK_a fit gives values of 6.2 $\pm$ 0.3 and 7.0 $\pm$ 0.2. A model compound for the reduced, aminoquinol form of cofactor has been synthesized and characterized (*21*). A comparison of the enzyme bound reduced topa cofactor (TPQ_{red}) and model compound deprotonation is illustrated in Figure 2. From the available copper amine oxidase crystal structures (*3*−*6*), a conserved aspartate is observed in the enzyme active site near the C-5 position of cofactor. This residue has been implicated as the active-site base in substrate oxidation (*3*, *7*) and is also expected to provide electrostatic stabilization to the sequence of positively charged intermediates of TPQ proposed to arise in the course of the reductive half-reaction (cf. Scheme 1). There are no other charged residues near the active-site aspartate, and the substrate pocket is lined with numerous hydrophobic residues. The anticipated proximity of the aminoquinol of reduced cofactor to the active-site aspartate side chain would, therefore, be expected to elevate the pK_a for ionization of the amino side chain in relation to the model compound (where pK_a = 5.9). This suggested that one of the kinetically measured pK_a values could reflect the ionization of the reduced cofactor.

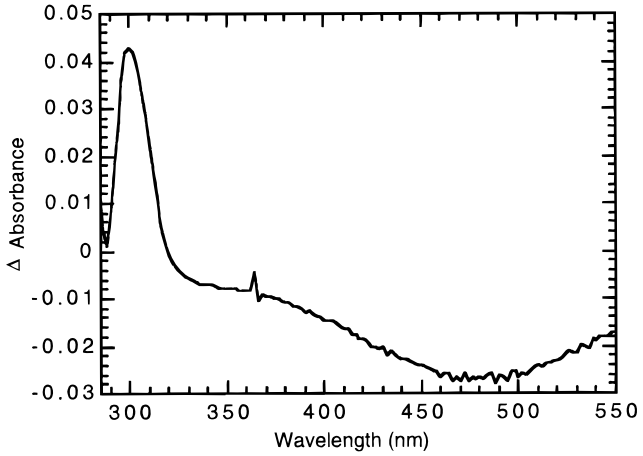

FIGURE 3: Difference UV−vis spectra of the BSAO reduced form minus the oxidized form.

Titration of the Reduced Enzyme. The UV−vis spectrum of anaerobically reduced BSAO was studied at different pH values. The spectrum of the resting enzyme has a characteristic absorption around 480 nm throughout the pH range from 5.5 to 9. Upon reduction, the 480 nm peak is bleached and a new peak around 300 nm appears. A typical difference spectrum of the reduced enzyme, compared to the native form, is shown in Figure 3. For the reduced enzyme, the absorbance at 300 nm is found to increase with increasing

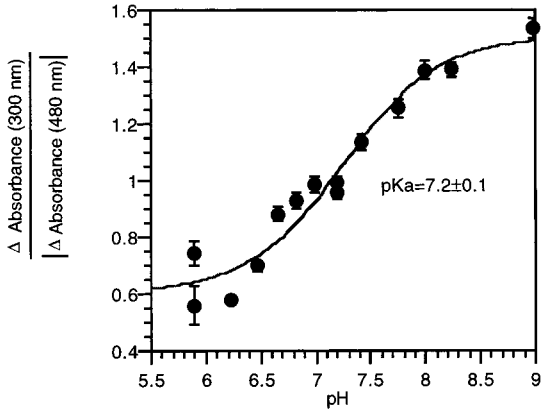

FIGURE 4: Titration of reduced BSAO. ΔAbsorbance (300 nm) is corrected for the BSAO concentration fluctuation reflected by |ΔAbsorbance| at 480 nm (see text). The line is a fit to the following equation: $\Delta\text{Absorbance} = \epsilon_1/(1 + 10^{\text{pH} - \text{p}K_a}) + \epsilon_2/(1 + 10^{\text{p}K_a - \text{pH}})$, where ϵ_1 and ϵ_2 are fitted constants reflecting different extinction coefficients at 300 nm for the protonated and deprotonated enzyme forms.

pH, while the absorbance at 480 nm remains unchanged. To quantitate the change in intensity at 300 nm, the pH-independent change in absorbance at 480 nm was used as an internal standard to correct for a slight fluctuation in enzyme concentration in different samples. The plot in Figure 4 thus shows the ratio of ΔAbsorbance (300 nm) to the absolute value of ΔAbsorbance at 480 nm at each pH. The data fit a single-proton dissociation equation, with a pK_a of 7.2 ± 0.1. This pK_a is within experimental error of the second pK_a determined from Figure 1. We therefore attribute pK_a(2) to the deprotonation of the reduced cofactor, while ascribing the lower pK_a to the ionization of a protein-bound functional group.

pH Dependence of Topa Semiquinone Formation. If the assignment of pK_a(2) from Figure 1 to reduced cofactor is correct, an effect of pH on other properties of the reducd cofactor is expected as well. It has been shown that the reduced cofactor in copper amine oxidases can undergo a one-electron transfer to the Cu(II) center, generating the Cu(I)−semiquinone complex (*13*). The semiquinone absorbance is seen at 465 nm in pea seedling amine oxidase (*14*) but is below the detection limit by UV−vis spectrophotometry for BSAO between pH 5.5 to 9. We therefore turned to EPR spectroscopy as a more sensitive probe of semiquinone formation in BSAO. Figure 5a shows EPR spectra for oxidized BSAO, indicating an essentially unchanged Cu(II) signal throughout the pH range. Figure 5b represents EPR spectra for the reduced BSAO under anaerobic conditions, where it can be seen that a new signal at g ∼2 appears with increasing intensity as the pH is elevated. The $g \sim 2$ signal is in the region anticipated for an organic radical and is assigned to the semiquinone radical. Because the level of semiquinone is quite low with a poor signal-to-noise ratio, a quantitative integration of the signal was not attempted. However, the data indicate a clear-cut trend of increasing semiquinone signal with increasing pH, supporting an ionization of the aminoquinol. The direction of the shift from Cu(II)−TPQ_{red} to Cu(I)−TPQ_{sq} with increasing pH is consistent with an expected increase in electron density and decrease in reduction potential as the reduced cofactor undergoes deprotonation.

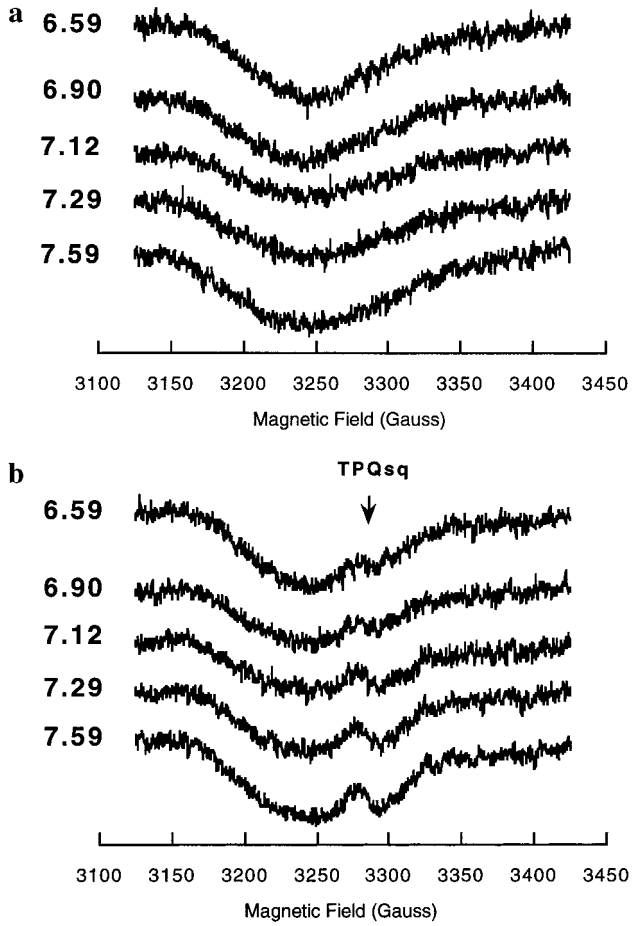

FIGURE 5: (a) EPR spectra of BSAO in the oxidized form. (b) EPR spectra of BSAO in the reduced form. pH values of the corresponding spectrum are indicated on the left of each spectrum. Parameters are described under Experimental Procedures.

Solvent Isotope Effect. Reduction of oxygen to hydrogen peroxide involves an uptake of two protons and two electrons. To establish whether any proton-transfer step is rate-limiting in the oxidative half-reaction, the solvent isotope effect on $V_{max}/K_m(O_2)$ was determined. $V_{max}/K_m(O_2)$ values were measured in D_2O over a range of pD values, and the pD profile was compared to the pH profile in H_2O (Figure 1). The $V_{max}/K_m(O_2)$ data in D_2O were also fit to a two pK_a deprotonation equation. The maximum value of $V_{max}/K_m(O_2)$ in D_2O is 1.15×10^5 M^{-1} s^{-1}, for comparison to a value of 1.21×10^5 in H_2O. The essentially equal values of $V_{max}/K_m(O_2)$ at the plateau indicate the absence of a kinetic solvent isotope effect, allowing us to rule out a proton-transfer step as rate-limiting in $V_{max}/K_m(O_2)$. This suggests that electron transfer and/or product dissociation are the slow steps in $V_{max}/K_m(O_2)$.

O-18 Kinetic Isotope Effect. The overall four-electron reduction of dioxygen to water leads to a range of oxygen intermediates that differ with regard to bond order. Thus, measurement of O-18 kinetic isotope effects in dioxygen reactions is expected to yield insight into, first, whether changes in bond order to dioxygen are kinetically significant and, second, the nature of the structural changes that are occurring at oxygen in the rate-determining step(s). Equilibrium O-18 isotope effects have been previously computed using literature values of frequencies and force constants for dioxygen, superoxide, and peroxide (*20*). These are repro-

Table 1: Calculated Equilibrium O-18 Isotope Effects and Reduction Potentials for the Intermediates in Dioxygen Reduction

reaction	O-18 EIE	reduction potential at pH 7 (v, vs NHE)[a]
$O_2 \overset{1e^-}{\rightleftharpoons} O_2^{\bullet -}$	1.0331[b]	−0.16[a]
$O_2 \overset{1e^-,1H^+}{\rightleftharpoons} HO_2^{\bullet}$	1.0115[b]	−0.29[c]
$O_2 \overset{2e^-,1H^+}{\rightleftharpoons} HO_2^-$	1.0340[b]	0.22[c]
$O_2 \overset{2e^-,2H^+}{\rightleftharpoons} H_2O_2$	1.0089[b]	0.36[a]
$HO_2^{\bullet} \overset{1e^-}{\rightleftharpoons} HO_2^-$	1.0222[d]	0.74[e]
$HO_2^{\bullet} \overset{1e^-,1H^+}{\rightleftharpoons} H_2O_2$	0.9974[d]	1.02[c]

[a] Sawyer (1991) *Oxygen Chemistry*, Oxford University Press, New York. [b] Tian and Klinman (1993) *J. Am. Chem. Soc. 115*, 8891. [c] Calculated from data in *a* based on the pK_a of $HO_2^{\bullet}$, 4.8 (ref *e*), and pK_a(1) of H_2O_2, 11.8 (ref *e*). [d] Calculated from data in *b*. [e] Hore (1985) *Standard Potentials in Aqueous Solution*, M. Dekker, New York.

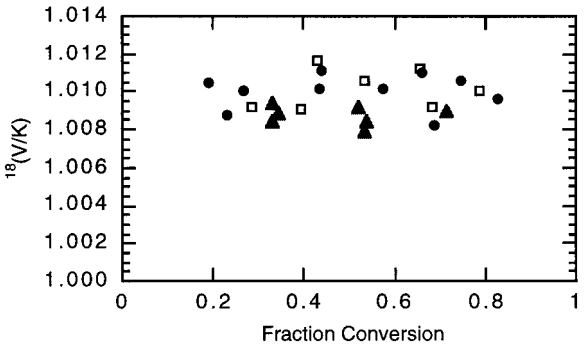

FIGURE 6: O-18 kinetic isotope effect. Data were acquired at pH 8.5 (circles), 7.2 (squares), and 6.0 (triangles).

duced in Table 1. A comparison of experimentally measured isotope effects in systems where oxygen interacts with a copper or iron ion as opposed to a proton suggests that substitution of a proton by a metal ion will yield values similar to those in Table 1 (*20*). This has been corroborated in subsequent computations of isotope effects using frequencies and force constants for iron−oxygen complexes (*22*). The measured O-18 kinetic isotope effects for BSAO are shown in Figure 6. $^{18}(V/K)$ is 1.0100 ± 0.0009, 1.0101 ± 0.0010, and 1.0087 ± 0.0005 for pH 8.5, 7.2, and 6.0, respectively. $^{18}(V/K)$ is essentially unchanged with pH, indicating that the rate-determining step occurs from the deprotonated form of enzyme and does not change with pH. The average value is 1.0097 ± 0.0010. This result shows clearly that changes in bond order to dioxygen are occurring in the rate-determining step of $V_{max}/K_m(O_2)$. As will be discussed below, the magnitude of $^{18}(V/K)$ is consistent with either a rate-limiting electron transfer to dioxygen to form a radical intermediate or a slow release of product hydroperoxide which is in a reversible equilibrium with dioxygen.

Viscosity Effect. The postulated mechanism for the oxidative half-reaction of the amine oxidases involves a one-electron transfer from reduced cofactor to the active-site Cu(II) to yield Cu(I)−semiquinone as the catalytically active species in dioxygen reduction (Dooley et al., 1991). The equilibrium isotope effect for formation of $HO_2^{\bullet}$ is 1.0115 (Table 1), providing an upper estimate for a kinetic isotope

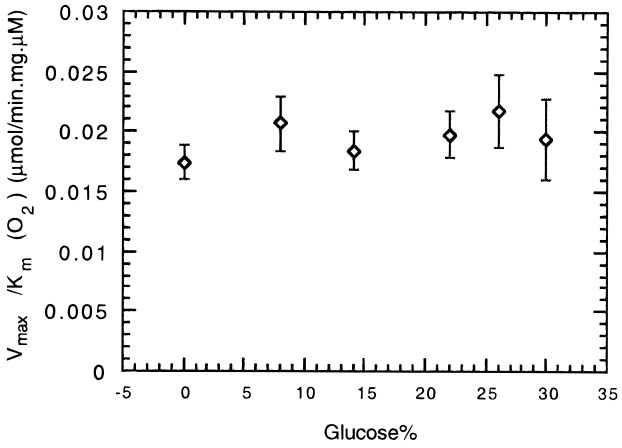

FIGURE 7: Effect of viscosogen concentration on $V_{max}/K_m(O_2)$.

Scheme 2: Initially Postulated Mechanism for Dioxygen Binding and Reduction at a Cu(I) Site

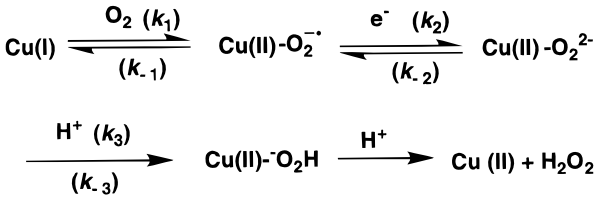

effect upon formation of a Cu(II)−superoxide complex. Since the experimentally observed $^{18}(V/K)$ is less than this equilibrium limit, a diffusional encounter between dioxygen and the Cu(I)−semiquinone form of enzyme to yield a Cu(II)−superoxide species could, in principle, represent the rate-limiting step in $V_{max}/K_m(O_2)$. This mechanism makes the prediction that $V_{max}/K_m(O_2)$ will be sensitive to solvent viscosogens. The $V_{max}/K_m(O_2)$ at various glucose concentrations was, therefore, determined at pH 6.5 (Figure 7). It can be seen that changes in viscosity have no effect on $V_{max}/K_m(O_2)$. We conclude that oxygen binding is not part of the rate-limiting step, that is, *that oxygen binding to enzyme and the electron transfer to oxygen are separate steps*. This rules out a mechanism in which a resting Cu(I) form of enzyme interacts directly with dioxygen in the rate-determining step.

We can also rule out a mechanism in which dioxygen binds reversibly to Cu(I) to form Cu(II)−superoxide, followed by a rate-limiting second electron transfer from cofactor, step 2 in Scheme 2. Under this assumption, an expression of microscopic rate constants and equilibrium constants for the steady-state parameter V/K can be deduced:

$$(V/K)^{-1} = (K_1K_2k_3)^{-1} + (K_1k_2)^{-1} + (k_1)^{-1} \qquad (4)$$

where K_1, K_2, and K_3 are equilibrium constants for steps 1, 2, and 3, respectively, and k_1, k_2, and k_3 are rate constants for steps 1, 2, and 3, respectively. If the second electron transfer (step 2 in Scheme 2) is the slow step, V_{max}/K_m is approximated by K_1k_2. The kinetic isotope effect is expected to lie between $^{18}(K_1)$ and $^{18}(K_1K_2)$, or the equilibrium isotope effects for Cu(II)−$O_2^{-\bullet}$ and Cu(II)−O_2^{2-}. Referring to Table 1, the two limits of $^{18}(V/K)$ are set to $1.0115 < {}^{18}(V/K) < 1.0340$. However, the observed $^{18}(V/K)$ is smaller than the expected lower limit for a slow second electron transfer, making step 2 an unsuitable candidate for the rate-limiting step in dioxygen reduction.

Scheme 3: Slow Peroxide Dissociation Mechanism

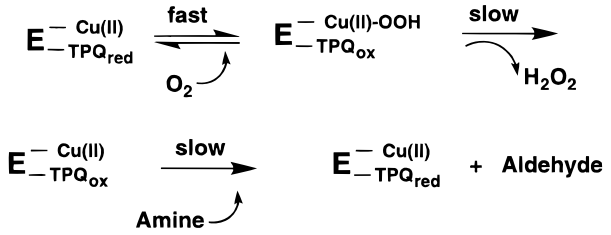

We further note that a mechanism in which a second electron transfer from cofactor to Cu(II)$-O_2^{\bullet-}$ to produce Cu(II)$-O_2^{2-}$ is the slow step appears highly unlikely based on reaction driving force. The estimated reduction potential for $HO_2^{\bullet}/HO_2^-$ (ca. 0.74 V (vs NHE), see Table 1) and for TPQ_{ox}/TPQ_{sq} (estimated as <0.1 V from the overall reduction potential of 0.1 V for the two-electron reduction of TPQ_{ox} to TPQ_{red} (vs NHE) (*21*), together with the observation that no intermediate semiquinone accumulates; the latter also indicates that the TPQ_{sq}/TPQ_{red} is >0.1 V) leads to an estimated $\Delta\epsilon^\circ > 0.64$ V for reduction of a copper superoxide to peroxide intermediate by TPQ_{red}. This contrasts with a strongly unfavorable driving force for the one-electron transfer from TPQ_{red} to dioxygen of less than -0.26 V (cf. Table 1 for the $O_2/O_2^{\bullet-}$ half potential of -0.16 V).

Is the Peroxide Release a Slow Step in $V_{max}/K_m(O_2)$? Another possible interpretation of the observed $^{18}(V/K)$ is that product hydroperoxide is formed reversibly from dioxygen and that release of bound peroxide represents the rate-limiting step for $V_{max}/K_m(O_2)$. The crystal structure for the *H. polymorpha* amine oxidase suggests that peroxide will dissociate into the extended water channel that occurs at the dimer interface (*6*). For this to occur, some movement of the side chain of Glu637 is required, raising the possibility of a kinetic barrier to peroxide release. This mechanism predicts an equilibrium isotope effect of 1.0089, within experimental error of the observed $^{18}(V/K)$. In the above analysis of O-18 kinetic isotope effect, there has been the working assumption that the second electron transfer to oxygen is an irreversible step. As no experimental data have been available addressing the reversibility of peroxide formation, the possibility of slow peroxide release was examined more closely.

Fast and reversible oxidation of the reduced BSAO by oxygen, followed by slow release of product peroxide, is shown in Scheme 3, where peroxide is illustrated as bound to the active-site Cu(II) (hydrogen peroxide could also be bound elsewhere in the active site, see below). According to Scheme 3, reaction of enzyme, that has been prereduced by amine substrate under anaerobic conditions, with oxygen in the presence of excess amine will lead to a fast equilibration of TPQ_{red} and TPQ_{ox}, prior to a further increase of TPQ_{ox} as peroxide dissociates and pulls the reaction forward. Since the redox potential of O_2/H_2O_2 [ϵ° (vs NHE) = 0.28 V at pH 7.0 (*23*)] is more positive than that of the TPQ_{ox}/TPQ_{red} [ϵ° (vs NHE) = 0.1 V at pH 7.0 in solution (*21*)], the initial, fast equilibration between TPQ_{red} and TPQ_{ox} is expected to favor the TPQ_{ox} form. We therefore would expect to see a burst of TPQ_{ox} formation, followed by a slow exponential increase of TPQ_{ox} as peroxide dissociates and pulls enzyme toward the steady-state level of TPQ_{ox}.

For illustrative purposes, this process was simulated using the program KINSIM and an assigned family of rate constants (see Appendix). Binding rate constants for amine and oxygen were set at the bimolecular encounter rate, $\sim 10^8$ M^{-1} s^{-1}, substrate off rates were calculated according to $k_{off} = k_{on}K_d$, where K_d is estimated using K_m values, and the rate of proton abstraction from amine was 2 s^{-1} (*24*). The magnitudes of deuterium isotope effects on $^D(V)$ and $^D(V/K)$ are given in Table 2. Since the isotope effect on $^D(V/K)$ reflects C$-$H bond cleavage (*24*), the reduced value for $^D(V)$ indicates that V_{max} is about half limited by C$-$ H abstraction and half limited by another step(s). Hydrolysis of the product Schiff base is concluded to be quite rapid, since all attempts to trap the product Schiff base have failed (*25*). Thus, the second slow step in V_{max} is expected to reside in the oxidative half-reaction and to have a similar rate to the proton abstraction rate. In this way, the peroxide decomposition rate was set to 3 s^{-1}, the rates of all proton-transfer and electron-transfer steps were set to 10^6 s^{-1}, and the rate of product Schiff base hydrolysis was set to 10^3 s^{-1}. The simulated result is shown in Figure 8, trace (a). The size of the burst depends on the equilibrium position of $E-TPQ_{red}-O_2 \rightleftharpoons E-TPQ_{ox}-H_2O_2$. Since equal rates have been set for the forward and reverse reactions of all steps, the equilibrium constant is unity in the simulation. As noted above, relative redox potentials suggest that the actual equilibrium constant would be larger than unity, so that the estimated burst in Figure 8a of 50% is likely to be a lower limit.

The possible validity of a mechanism in which a slow release of peroxide limits $V_{max}/K_m(O_2)$ was then tested by monitoring the rate of TPQ_{ox} formation upon mixing BSAO, reduced anaerobically by amine, with oxygen under condi-

Table 2: Steady-State Kinetic Parameters and Deuterium Isotope Effects[a]

substrate	V_{max} (unit/mg)	V/K (unit/mg·mM)	^DV	$^D(V/K)$
[1,1-$^1H_2$] benzylamine	0.29 ± 0.01	0.055 ± 0.004	6.0 ± 0.3	10.0 ± 0.8
[1,1-$^2H_2$] benzylamine	0.048 ± 0.002	0.0055 ± 0.0005		

[a] Data were collected at pH 6.5, in 100 mM potassium phosphate buffer, ionic strength 0.3 M.

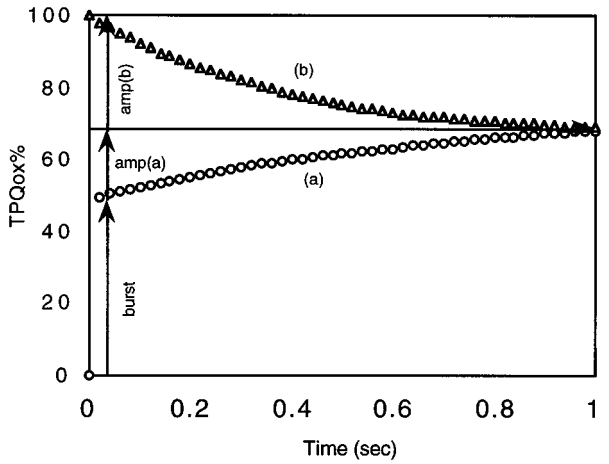

FIGURE 8: Simulation of the change in TPQ_{ox} concentration according to Scheme 3. (a) BSAO starts as the reduced form and reacts with excess oxygen in the presence of saturated amine; (b) BSAO starts as the oxidized form and reacts with excess amine in the presence of saturated oxygen.

Table 3: Aerobic and Anaerobic (quasi) Stopped-Flow Results[a]

process	amplitude of A_{480}	E−TPQ_{ox}/E_{total} (%)
aerobic E-TPQ_{ox} + [1,1-$^1H_2$] benzylamine → steady-state	0.0106 ± 0.0002	58
anaerobic (quasi) E-TPQ_{red} + O_2 → steady-state	0.0145 ± 0.0011	58
aerobic E-TPQox + [1,1-$^2H_2$] benzylamine → steady-state	0.0014 ± 0.0002	94

[a] Conditions are described in Experimental Procedures under Stopped-Flow Kinetics.

tions of stopped-flow spectrophotometry. A single exponential increase of A_{480} with an amplitude of 0.0145 ± 0.011 was seen (Table 3). The absence of a burst phase appeared to eliminate the mechanism in Scheme 3. However, due to the difficulty of establishing a highly precise baseline in the stopped flow, it remained possible that a burst existed but that it had been lost in the dead time of the instrument. This problem was solved by analyzing the approach to the steady state in the stopped flow starting with oxidized BSAO that was mixed aerobically with a saturated amine solution; in this case the loss of A_{480} was monitored. This process is expected to reach the same steady-state level of TPQ_{ox} as the reaction of TPQ_{red} with oxygen, Figure 8b. In the event of a burst phase which is within the dead time of the instrument, a slow peroxide release mechanism will lead to a sum of amplitudes from the exponential traces which is less than the total TPQ concentration (with the difference being the burst phase). The decrease of A_{480} in the stopped-flow experiment beginning with TPQ_{ox} also shows a single-exponential trace with an amplitude of 0.0106 ± 0.0002 (Table 3). Importantly, the sum of the amplitudes from the two observed processes is 0.0251, essentially equal to the calculated (0.028) and experimentally measured change in absorbance at 480 nm following conversion of 21.15 μM BSAO from its oxidized to reduced state (0.025 ± 0.01). This result shows that there is no burst of TPQ_{ox} formation following reaction of dioxygen with anaerobically reduced BSAO, that is, that the E−TPQ_{red}−O_2 complex is quantitatively converted to E−TPQ_{ox}−H_2O_2 in the presence of dioxygen. A reversible formation of E−TPQ_{ox}−H_2O_2 followed by a rate-limiting release of hydrogen peroxide is therefore ruled out as the mechanism for $V_{max}/K_m(O_2)$. By contrast, simulations of mechanisms which involve a slow one-electron transfer to enzyme-bound dioxygen are consistent with the observed stopped-flow results. We note that rate-limiting formation of a superoxide intermediate has previously been seen in oxygen reduction by flavin (*26*) and pterin (*27*) cofactors.

Rate-Limiting Steps in V_{max}. Two steps (at a minimum) contribute to V_{max}: one from the reductive half-reaction and one or more from the oxidative half-reaction. From the size of the substrate deuterium isotope effect, a proton abstraction from C-1 of substrate within the substrate Schiff base complex arises from the reductive half-reaction and contributes to V_{max}. A slow electron transfer from TPQ_{sq} to superoxide is ruled out since no accumulation of TPQ_{sq} signal was observed during the steady-state reaction. This leaves the first electron transfer from TPQ_{red} to dioxygen, together

Scheme 4: Summary of Enzyme Forms in the Steady State under Conditions of Saturation with Substrate and Dioxygen: Species that Precede the Slow Steps Will Accumulate

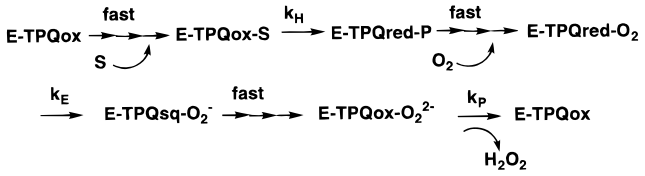

with the proton transfer to peroxide and the release of bound peroxide, as possible contributing steps to V_{max}. Although the amplitudes of observed stopped-flow traces (Table 3) preclude a reversible formation of bound peroxide followed by a slow product release step, it was feasible that a slow proton transfer or a slow release of hydrogen peroxide was occurring after the irreversible electron-transfer steps. The question of another slow step in V_{max} after the two electron transfers to dioxygen was addressed through an analysis of the steady-state distribution of enzyme species using the deuterium isotope effects on V_{max} and V_{max}/K_m(amine) (Table 2). The isotope effect, ^DV of 6.0 ± 0.3, is interpreted as

$$k_{cat}(H) = 6k_{cat}(D) \quad (5)$$

where k_{cat}(H) is the k_{cat} for the protonated substrate, while k_{cat}(D) is the k_{cat} for the deuterated substrate. $^D(V/K)$ of 10.0 ± 0.8 is the deuterium isotope effect on proton abstraction, which reflects a single C−H bond cleavage step. Thus:

$$k_H = 10k_D \quad (6)$$

We can, therefore, write

$$1/k_{cat}(H) = 1/k_H + 1/k_2 \quad (7)$$

$$1/k_{cat}(D) = 1/k_D + 1/k_2 \quad (8)$$

where k_2 contains the rate constant(s) for the slow step(s) in the oxidative half-reaction. Solving eqs 5−8, the ratio of k_H/k_2 is obtained as 4/5. Assigning $k_H = 4x$, we have $k_2 = 5x$. From the analysis of $V_{max}/K_m(O_2)$, we assign the first electron transfer to O_2 as one of the rate-limiting steps in the oxidative portion of V_{max} and also allow the peroxide protonation and/or release step to be slow and partially rate-limiting. We then write

$$1/k_2 = 1/k_E + 1/k_P = 1/5x \quad (9)$$

where k_E is the rate constant for the first electron transfer, while k_P is the combined rate constant for the subsequent step(s).

In the steady state of BSAO, under conditions of saturating substrate and dioxygen, those intermediates that precede slow steps will accumulate. These are shown in Scheme 4 as the substrate Schiff base (E−TPQ_{ox}−S), the complex of reduced enzyme with O_2 (E−TPQ_{red}−O_2), and the oxidized enzyme complexed with peroxide (E−TPQ_{ox}−O_2^{2-}). $1/k_H$ reflects the time the enzyme retains the E−TPQ_{ox}−S form due to slow proton abstraction, while $1/k_E$ reflects the E−TPQ_{red}−O_2 retention time due to slow electron transfer, and $1/k_P$ reflects the E−TPQ_{ox}−O_2^{2-} retention time due to any slow step after both electrons are transferred to dioxygen. The

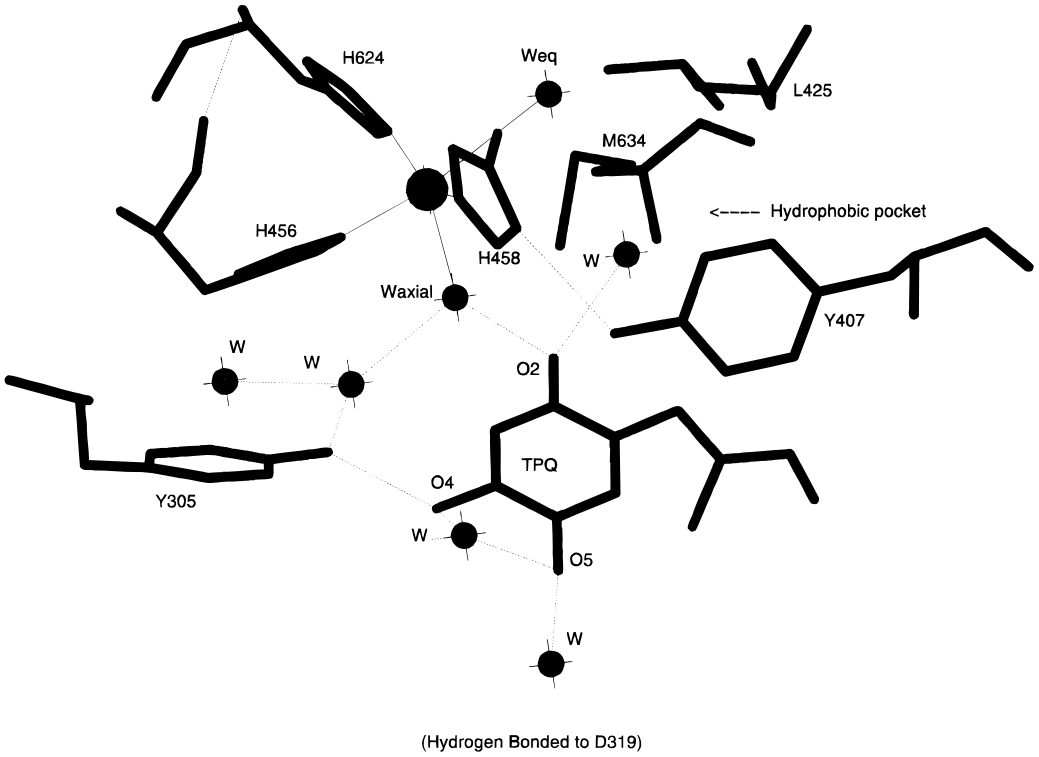

FIGURE 9: The active site of HPAO. TPQ (at bottom of the figure) is separated from the copper site (at top left of the figure) by Y305 and Y407. The proposed hydrophobic pocket (on the right of the figure) is composed of Y407, M634, and L425. Waters are depicted as balls and labeled with "W". W_{axial} and W_{eq} represent the axial and equatorial water of copper, respectively. Dashed lines indicate hydrogen bonds. Solid lines indicate copper−ligand interactions.

steady-state concentration of each enzyme species is directly proportional to its retention time. This allows correlation of the rate constants with the steady-state $E-TPQ_{ox}$ level (given in Table 3)

$$E-TPQ_{ox}/E_{Total} = (1/k_H + 1/k_P)/(1/k_H + 1/k_E + 1/k_P) = 0.58 \quad (10)$$

Combining eqs 7, 9, and 10, k_P and k_E can be solved as $91x$ and $5.3x$, respectively. This result indicates that practically all of the oxidized form of enzyme that accumulates during the steady state can be attributed to the $E-TPQ_{ox}-S$ species. We conclude that in the oxidative half-reaction, all steps after formation of oxidized TPQ are fast, leaving the first electron transfer as the only rate-limiting step in the oxidative half-reaction of V_{max} (representing approximately 40% of the overall rate limitation in V_{max}).

Since deuterated substrate slows down k_H without affecting other steps, the $E-TPQ_{ox}$ concentration at steady state should be much different with deuterated amine. The expected $E-TPQ_{ox}$ level using deuterated substrate is

$$E-TPQ_{ox}/E_{Total} = (1/k_D + 1/k_P)/(1/k_D + 1/k_E + 1/k_P) \quad (11)$$

Substituting k_D with $4x/10$, k_P with $91x$, and k_E with $5.3x$, $E-TPQ_{ox}/E_{Total}$ is calculated to be 0.93. The steady-state $E-TPQ_{ox}$ concentration using 1,1-$^2H_2$ benzylamine was observed to be 94% (Table 3), in full support of the assignment of the rate-limiting steps in V_{max} to k_H and k_E.

DISCUSSION

Crystal structures are currently available for TPQ-containing copper amine oxidase from four sources: *E. coli* (*3*), *pea seedlings* (*4*), *A. globiformis* (*5*), and *H. polymorpha* (*6*). In contrast to the earlier structures, the recently solved structure for the copper amine oxidase from *H. polymorpha* shows the cofactor to be fixed in position and oriented as anticipated for catalysis, with the C-5 carbonyl of cofactor pointing toward the amine binding pocket and the active-site base in position for assisting Schiff base formation (cf. Scheme 1). As illustrated in Figure 9, the TPQ cofactor essentially bifurcates the active site, with the active-site base and substrate binding pocket cut off from the copper binding site by two tyrosine residues (Tyr 305 and 407) that lie above and below the cofactor. Communication between the two halves of the active site occurs via an extensive network of hydrogen bonding that involves the active-site base, Tyr 305, and numerous waters that include the axial and equatorial waters complexed to the cupric ion. We think of the TPQ cofactor as a "transducer", storing two electrons and two protons for later delivery to molecular oxygen. Both of the electrons and one of the protons (at O-4 of reduced cofactor) have been proposed to arise from substrate (*28*), while the proton at O-2 of reduced cofactor has been postulated to come from the axial water complexed to cupric ion (*29*).

In this work we have attempted to elucidate the mechanism whereby these two protons and electrons are transmitted from reduced cofactor to molecular oxygen in the production of H_2O_2. A multifaceted kinetic approach has combined the measurement of pH dependencies, solvent and oxygen-18 isotope effects, and solvent viscosity effects to gain insight into the nature of the rate-determining step of dioxygen reduction. One curious feature of the BSAO oxidative half-reaction is that while the reduction of dioxygen to hydrogen peroxide requires two protons, the steady-state pH dependence study reveals that two groups must be deprotonated

for the oxidative-half-reaction to proceed. This implies that the pK_a's from $V_{max}/K_m(O_2)$ are due to groups that are different from those that serve as proton sources for dioxygen reduction. From a comparison of the pH dependencies of $V_{max}/K_m(O_2)$ to the pH dependence of the formation of reduced cofactor, it has been possible to assign a pK_a of 7.2 to the reduced aminoquinol form of TPQ, which must be deprotonated to its neutral form for catalysis. Such deprotonation will lower the redox potential for cofactor reoxidation (*21*). The pK_a for cofactor is significantly elevated relative to that in solution, consistent with the presence of an anionic active-site base that provides electrostatic interaction with the protonated cofactor (Figure 2). The second pK_a of 6.2 that controls $V_{max}/K_m(O_2)$ is not well-defined from this study. Given the extended hydrogen-bonding network that defines the active site, this could reflect an ionization of one of the copper-bound waters. The axial water to copper has been postulated to be a proton donor in the conversion of TPQ_{ox} to TPQ_{red} (*29*). Maintenance of this axial water as a hydroxide ion during the oxidative half-reaction may modulate the interaction of the equatorial water with the cupric site. As discussed below and in Li et al. (*6*), the equatorial water lies near a postulated dioxygen binding site. The pK_a of Cu(II)-bound water in aqueous solution is 7.53 (*30*). Within the active site of BSAO, this pK_a could be lowered to 6.2 as a result of the ligands to the copper center and the presence of directed hydrogen bonds for charge stabilization of the resulting metal-bound hydroxide. We note that no comparable pK_a has yet been seen in the pH dependence of V_{max}/K_m for substrate (*28*), suggesting that the pK_a of metal-bound water in oxidized enzyme would be perturbed to a value outside the experimental pH range.

Our initial working hypothesis for the reduction of molecular oxygen stemmed from the finding of Dooley and co-workers that reduced copper amine oxidases undergo an intramolecular electron transfer to yield cuprous ion and the semiquinone of TPQ (cf. Scheme 2). Thus, dioxygen was originally expected to interact with Cu(I), leading to Cu(II)−superoxide as the first intermediate in $V_{max}/K_m(O_2)$. The absence of any solvent isotope effects rules out proton transfer as contributing to $V_{max}/K_m(O_2)$ (Figure 1), whereas the oxygen-18 isotope effects indicate quite clearly that electron transfer to dioxygen is a rate-limiting step in $V_{max}/K_m(O_2)$ (Figure 6). Two plausible mechanisms were proposed involving either a slow one-electron transfer to molecular oxygen or a reversible formation of enzyme-bound hydrogen peroxide followed by a slow release of peroxide from the enzyme. The stopped-flow studies (Figure 8 and Table 3) rule out the latter possibility, leading to the conclusion that conversion of dioxygen to superoxide is limiting $V_{max}/K_m(O_2)$. One key feature of Scheme 2 is that electron transfer from Cu(I) to dioxygen is expected to occur concomitantly with dioxygen binding, that is, it is very difficult to conceive of a productive interaction between Cu(I) and dioxygen that prevents a transfer of electron density to the oxygen, followed by a rate-limiting step that involves one-electron reduction of dioxygen to superoxide. If O_2 binding and reduction occur simultaneously, $V_{max}/K_m(O_2)$ for BSAO is expected to be sensitive to solvent viscosity. However, as seen in Figure 7, $V_{max}/K_m(O_2)$ is independent of an increase in solvent viscosity. *This key result indicates that oxygen binding to enzyme must occur in a step separate from its one-electron reduction to molecular oxygen, ruling out the mechanism in Scheme 2 as the pathway for oxygen activation.*

Scheme 5: Proposed Mechanisms for Dioxygen Binding and Reduction at the Hydrophobic Pocket: (a) Superoxide Moves onto Cu(II); (b) Superoxide Remains in the Initial O_2 Binding Pocket

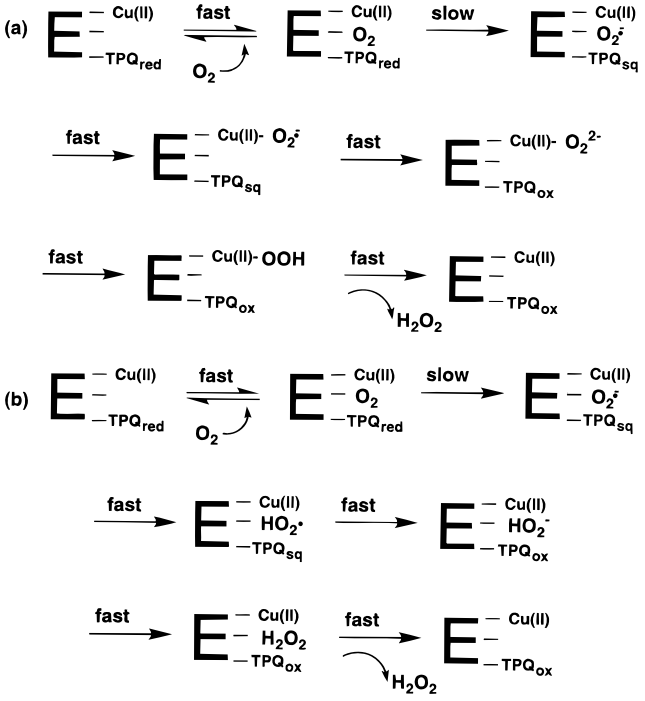

Where then does O_2 bind if not to the active-site copper ion? It is well-known that O_2 has hydrophobic character, partitioning into a hydrophobic phase from an aqueous phase in the ratio of 5−10:1 (*31*). From a recently completed crystallographic study of the *H. polymorpha* copper amine oxidase, it has been possible to identify a hydrophobic site that is near the equatorial water and contains an additional water that is hydrogen bonded to the O-2 oxygen of the (resting, oxidized) cofactor. The occupancy of this site by water is somewhat less than that seen for the majority of the other conserved waters observed in the active site [the water near O-2 is seen in 4 out of 6 of the subunits in the crystallographic asymmetric unit with a B factor of 45 Å^2 (*6*)]. As shown in Figure 9, this site is comprised of a Tyr (407), a Met (634), and a Leu (425). A linear alignment of the *H. polymorpha* sequence with the 10 other sequenced copper amine oxidases indicates that Tyr 407 is conserved in *E. coli*, *Klebsiella pneumoniae*, *A. globiformis*, *Arthrobacter* strain P1, bovine serum, human kidney, and human placental; Met 634 is seen in pea seedling, lentil seedling, *E. coli*, *K. pneumoniae*, *A. globiformis*, and *Arthrobacter* strain P1; and Leu 425 is seen in pea seeding and lentil seedling. In the case of BSAO, these residues are Tyr, Thr, and Ala.

Our final mechanism for the oxidative half-reaction of BSAO is shown in Scheme 5. Dioxygen is proposed to bind in a designated site near the O-2 position of TPQ. The reduced TPQ initiates the reaction by transferring one electron to dioxygen to form the superoxide ion. The designation of this first electron transfer as the rate-limiting step is consistent with the negative redox potential for the

formation of superoxide anion at pH 7 (−0.16 V) in relation to the estimated potential for TPQ_{sq}/TPQ_{red} of >0.1 V. Although redox potentials for species in solution suggest that the first electron transfer from TPQ_{red} to O_2 is highly unfavorable thermodynamically, the formation of superoxide anion in the enzyme active site may be significantly stabilized by its proximity to a positive charge induced upon TPQ semiquinone formation ($TPQ_{sq}^{\bullet+}$), as well as the presence of neighboring hydrogen bonds and a cupric ion. We note that the equilibrium isotope effect for the formation of superoxide anion from dioxygen is 1.0331, which sets an upper limit for the kinetic isotope effect. The fact that the observed isotope effect is much reduced from 1.0331 indicates either that the electron-transfer step is not fully rate determining (i.e., it is possible that there is a partially rate determining conformational change that precedes the electron transfer) or that $O_2^{\bullet-}$ is interacting with residues in the active site that increase its bond order. The latter could be due to some interaction with the cupric ion site as $O_2^{\bullet-}$ is formed. It is not possible to interpret the size of O-18 isotope effects for a single, rate-limiting electron-transfer step in terms of simple transition-state theory. It is expected that the electron will tunnel from TPQ_{red} to O_2 and that the rate of this tunneling is controlled by the unfavorable reaction driving force and the Franck−Condon barrier. In the event of an interaction of the superoxide ion with copper, some reorganization of the copper ligands (in particular the equatorial water, Figure 9) would be required and, as such, could also contribute to the reaction barrier for the first electron-transfer step. A copper-bound superoxide would subsequently undergo a series of rapid steps involving second electron, first proton, and second proton transfers, followed by peroxide dissociation into the water channel at the dimer interface (Scheme 5a).

One feature of coupled proton and electron-transfer processes is that while electrons can move (tunnel) over long distances, proton movement is restricted to a distance of no more than 1 Å. Valuable insight into the proton-transfer events comes from tracing the source of the two protons that end up in the hydrogen peroxide product. The C-1 proton of the amine substrate is abstracted by the aspartate and postulated to be placed at the O-4 of the reduced TPQ (*28*); this O-4 proton is lost upon reoxidation of TPQ (*28*) and is almost certainly one of the protons transferred to dioxygen during the oxidative half-reaction. Reduction of TPQ_{ox} converts O-2 from a carbonyl oxygen to an oxyanion with a pK_a of around 10 (*21*). The HPAO structure indicates a hydrogen bond between the axial water on copper and O-2 in the resting enzyme, which is therefore expected to be converted to copper hydroxide and protonated reduced cofactor. Thus, the second proton is very likely to come from O-2 of TPQ_{red}. In the structure of HPAO (*6*), O-4 of the TPQ is hydrogen bonded to a conserved tyrosine residue Y305, and this tyrosine residue is connected to the axial water of the copper site through another water molecule. Position O-2 of the TPQ is also hydrogen bonded to the axial water of copper and to another water in the postulated O_2 binding site. How would protons arrive at reduced oxygen if superoxide is bonded directly to the copper ion? One possibility is that the equatorial water moves into the position originally occupied by dioxygen and serves as a conduit for proton transfer via the O-2 position of cofactor. As an alternative, end-on binding of peroxide to Cu(II) by the σ donor interaction of the O_2^{2-} π_σ^* orbital with Cu(II) $d_{x^2-y^2}$ (*32*) might orient the O−O bond perpendicular to the Cu−O bond and the free end of oxygen about 3 Å from the axial water oxygen. In this case, the axial water could be positioned to pass both protons from the cofactor to the copper-peroxy species.

Given the implication of a hydrophobic binding pocket for dioxygen that is separate from the copper site, together with the evidence for a rate-limiting one-electron transfer from reduced cofactor to dioxygen, it is also possible that the subsequent rapid transfer of an electron and two protons from the cofactor semiquinone to superoxide to yield TPQ_{ox} and H_2O_2 could proceed without a migration of reduced oxygen intermediates to the copper center (Scheme 5b). Following a rate-limiting formation of superoxide ion, this intermediate would be perfectly positioned for further protonation and reduction by cofactor. The first proton transfer from the O-2 position of cofactor to $O_2^{\bullet-}$ would yield (the stabilized) protonated superoxide. Reprotonation of the O-2 position of cofactor is visualized as occurring via the hydrogen-bonded network that links the O-4 and O-2 positions of cofactor (Figure 9), leading to deprotonation at O-4 and protonation at O-2. At this stage, the cofactor would be a neutral semiquinone. Subsequent electron and proton transfer to $HO_2^{\bullet}$ would produce bound hydrogen peroxide, which could exit the active site via a route similar to that for O_2 entry. As a hybrid mechanism between this "copper off" mechanism (Scheme 5b) and the one described above in which superoxide anion moves to the copper site (Scheme 5a), we also considered the possibility that an intermediate peroxy anion (HO_2^-) migrated to the copper site. Although it is impossible to rule out such an event, it seems catalytically counterproductive to move a hydroperoxy-anion from a site where it is positioned for proton uptake to a copper site from which it must dissociate prior to the second proton transfer that leads to H_2O_2.

A surprising feature of the final mechanism in Scheme 5 is the passive role played by the cupric ion in catalysis. It is proposed that copper plays a multifaceted role which involves electrostatic stabilization of reduced oxygen intermediates either at a distance (Scheme 5b) or by direct binding of superoxide anion (Scheme 5a), as well as serving as the "mortar" for an extensive hydrogen-bonded network that moderates proton-transfer rates and pK_a values for the cofactor and copper-bound water. The ability to carry out the full catalytic cycle without reduction of cupric to cuprous ion has a distinct advantage of removing major ligand reorganization steps from the energy profile. Unlike other copper proteins that must cycle between Cu(II) and Cu(I) for effective catalysis, the quinocofactor in the copper amine oxidases has the capacity for redox cycling in the absence of involvement of a redox-active metal center (*21*). There is still debate in the literature as to whether the oxidative half-reaction of the copper amine oxidase can proceed at all in the absence of active-site metal or by replacement of the copper by other redox-inactive metal centers (*12, 33*). There is, however, no question regarding the essentiality of copper in the biogenesis of the TPQ from its precursor Tyr, which has been shown to be inert in the absence of copper (*5, 34*) or upon replacement of copper by zinc ion (*34*). Nonethe-

less, despite the critical role played by copper ion in TPQ biogenesis, there is still no formal proof for reduction of Cu(II) to Cu(I) in this process. In fact, Williams and Klinman have recently proposed a biogenesis mechanism that proceeds via a charge-transfer complex of Cu(II) and a tyrosinate ion without the necessity to generate Cu(I) and tyrosyl radical as discrete precursor species (*35*).

ACKNOWLEDGMENT

We thank Professor Jack F. Kirsch for kindly providing access to the stopped-flow instrument, Professor Yeon Kyun Shin for kindly allowing use of the EPR spectrometer, Wenzhong Xiao for assistance with the EPR spectrometer, Professor Frank M. Raushel (Texas A & M University) for kindly providing the SGI version of KINSIM, and Dr. Xuefei Sophie Wang for generously providing the enzyme.

APPENDIX

Simulation of Stopped-Flow Traces. The trace of the E−TPQ_{ox} concentration change upon mixing of the enzyme with amine and dioxygen under saturation conditions was simulated using an SGI version of KINSIM. The detailed mechanism applied was as follows:

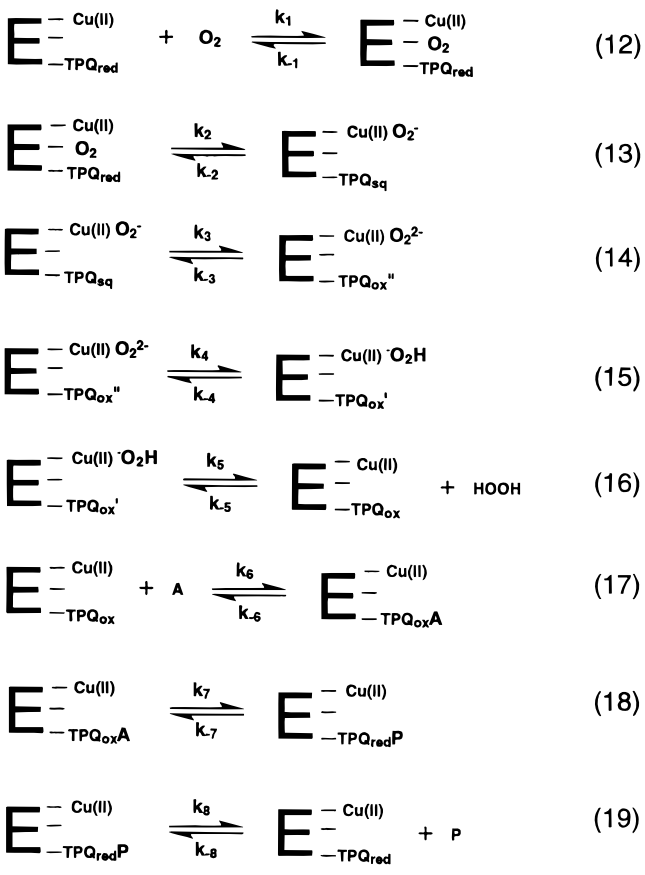

The simulation calculates the total concentration of the oxidized enzyme forms, which is the sum of all enzyme species containing TPQ_{ox}. The microscopic rate constants used in the simulation for the case of a rapid electron-transfer equilibrium followed by slow peroxide release are listed in Table 4.

Table 4: Microscopic Rate Constants Used in Simulation for the Case Where Peroxide Dissociation is the Slow and First Irreversible Step in the Oxidative Half-Reaction

k_1	1×10^8 M^{-1} s^{-1}	k_{-1}	1×10^3 s^{-1}
k_2	1×10^6 s^{-1}	k_{-2}	1×10^6 s^{-1}
k_3	1×10^6 s^{-1}	k_{-3}	1×10^6 s^{-1}
k_4	1×10^6 s^{-1}	k_{-4}	1×10^6 s^{-1}
k_5	3 s^{-1}	k_{-5}	0 s^{-1}
k_6	1×10^8 M^{-1} s^{-1}	k_{-6}	4×10^5 s^{-1}
k_7	2 s^{-1}	k_{-7}	0 s^{-1}
k_8	1×10^3 s^{-1}	k_{-8}	0 s^{-1}

REFERENCES

1. Oi, S., Inamasu, M., and Yasunobu, K. T. (1970) *Biochemistry 9*, 3378−3383.
2. Janes, S. M., Mu, D., Wemmer, D., Smith, A. J., Kaur, S., Maltby, D., Burlingame, A. L., and Klinman, J. P. (1990) *Science 248*, 981−987.
3. Parsons, M. R., Convery, M. A., Wilmot, C. M., Yadav, K. D. S., Blakeley, V., Corner, A. S., Philips, S. E. V., McPherson, M. J., and Knowles, P. F. (1995) *Structure 3*, 1171−1184.
4. Kumar, V., Dooley, D. M., Freeman, H. C., Guss, J. M., Harrey, I., McGuirl, M. A., Wilce, M. C. J., and Zubak, V. M. (1997) *Structure 4*, 943−955.
5. Wilce, M. C. J., Dooley, D. M., Freeman, H. C., Guss, J. M., Matsunami, H., McIntire, W. S., Ruggiero, C. E., Tanizawa, K., and Yamaguchi, H. (1997) *Biochemistry 36*, 16116−16133.
6. Li, R., Klinman, J. P., and Mathews, F. S. (1998) *Structure 6*, 293−307.
7. Plastino, J., and Klinman, J. P. (manuscript in Preparation).
8. Hartmann, C., and Klinman, J. P. (1991) *Biochemistry 30*, 4605−4611.
9. Klinman, J. P., and Mu, D. (1994) *Annu. Rev. Biochem. 63*, 299−344.
10. Younes, M., and Weser, U. (1978) *Biochim. Biophys. Acta 526*, 644−647.
11. Dooley, D. M., Cote, C. E., and Golnik, K. C. (1984) *J. Mol. Catal. 23*, 243−253.
12. Suzuki, S., Sakurai, T., Nakahara, A., Manabe, T., and Okuyama, T. (1983) *Biochemistry 22*, 1630−1635.
13. Dooley, D. M., McGuirl, M. A., Brown, D. E., Turowski, P. N., McIntire, W. S., and Knowles, P. F. (1991) *Nature 349*, 262−264.
14. Turowski, P. N., McGuirl, M. A., and Dooley, D. M. (1993) *J. Biol. Chem. 268*, 17680−17682.
15. Summers, M. C., Markovic, R., and Klinman, J. P. (1979) *Biochemistry 18*, 1969−1979.
16. Yasunobu, K. T., Ishitaki, H., and Minamiura, N. (1976) *Mol. Cell. Biochem. 13*, 3.
17. Bardsley, W. G., Crabbe, M. J. C., and Shinder, J. S. (1973) *Biochem. J. 13*, 459.
18. Schowen, B., and Schowen, R. L. (1982) *Methods Enzymol. 87*, 551−606.
19. Weast, R. C., Astle, M. J., and Beyer, W. H. (1983−1984) *CRC Handbook of Chemistry*, 64th ed., CRC Press, Boca Raton, FL.
20. Tian, G., and Klinman, J. P. (1993) *J. Am. Chem. Soc. 115*, 8891−8897.
21. Mure, M., and Klinman, J. P. (1993) *J. Am. Chem. Soc. 115*, 7117−7127.
22. Burger, R. M., Tian, G., and Drlica, K. (1995) *J. Am. Chem. Soc. 117*, 1167−1168.
23. Sawyer, D. T. (1991) *Oxygen Chemistry*, Oxford University Press, New York.
24. Palcic, M. M., and Klinman, J. P. (1983) *Biochemistry 22*, 5957−5966.
25. Hartmann, C., and Klinman, J. P. (1987) *J. Biol. Chem. 262*, 962−965.

26. Kemal, C., Chan, T. W., and Bruice, T. C. (1977) *J. Am. Chem. Soc. 99*, 7272−7286.
27. Eberlein, G., Bruice, T. C., Lazarus, R. A., Henrie, R., and Benkovic, S. J. (1984) *J. Am. Chem. Soc. 106*, 7916−7924.
28. Farnum, M., Palcic, M., and Klinman, J. P. (1986) *Biochemistry 25*, 1898−1904.
29. Klinman, J. P. (1996) *Chem. Rev. 96*, 2541−2561.
30. Yatsimirksii, K. B., and Vasil′ev, V. P. (1960) *Instability Constants of Complex Compounds*, Pergamon Elmsford, New York.
31. Sawyer, D. T., Chiericato, G. J., Angelis, C. T., Nanni, E. J., Jr., and Tsuchiya, T. (1982) *Anal. Chem. 54*, 1720−1724.
32. Solomon, E. I., Hemming, B. L., and Root, D. E. (1993) *Bioinorganic Chemistry of Copper*, Chapman & Hall, New York.
33. Agostinelli, E., Morpurgo, L., Wang, C., Giartosio, A., and Mondovi, B. (1994) *Eur. J. Biochem. 222*, 727−732.
34. Cai, D. Y., Williams, N. K., and Klinman, J. P. (1997) *J. Biol. Chem. 272*, 19277−19281.
35. Williams, N., and Klinman, J. P. (1998) (in Press). †This research was supported by grants from the National Institutes of Health, GM 39296 and GM 25765.

BI981103L